

Mountain Valley Evacuation by Upper Level Flows: A Scale Model Study

William J. Cunningham Jr.*
University of Colorado, Boulder, Colorado 80309
and

Alfred J. Bedard Jr.†
*National Oceanic and Atmospheric Administration/Environmental Research Laboratories,
Boulder, Colorado 80303*

The motivation for this study was to understand the complex shear flow associated with the evacuation of inversion layers and the removal of pollution from mountain valleys. An upper level flow across an inversion layer within a mountain valley can create strong wind shear and turbulence at the inversion interface. In our experiments, the inversion layer was forced over the downstream mountain followed by the establishment of a new steady-state equilibrium position for the inversion. The evacuation process was dependent on the onset of a standing wave in the mountain valley and the formation of a vortex on the leeside of the upstream mountain. This phenomenon only occurred at higher flow velocities. Subsequently, the inversion layer was no longer forced over the downstream mountain, but drawn up the leeside of the upstream mountain by the vortex and transported away by the upper level flow. This situation has important implications for airports in mountainous regions, suggesting it may be feasible to predict the onset and time scale of the erosion process. We include comparisons with atmospheric flows.

Introduction

THERE have been studies of the interaction between flows aloft and cool, stable air trapped by valleys. Laboratory¹ and combined numerical/laboratory² results, as well as field measurements,^{3,4} indicate that the Froude number can be used as an index to determine the start of the erosion process of the cool air pool. However, the erosion process can be expected to be more complex because of the combined effects of valley flow oscillations and instabilities related to flow separation near a mountaintop. These possibilities were suggested by Neff and Ruffieux.⁵ Our laboratory experiments focused on defining the types and sequences of physical processes that dominate the erosion process.

We performed the scale model experiments in a water tunnel at the University of Colorado. We used mathematically defined forms for the valley model hoping that these laboratory model experiments will provide a resource for comparison with numerical models. For example, Durran⁶ has used a "Witch of Agnesi" mountain profile in his numerical simulations. We combined two Witch of Agnesi mountain profiles in creating the valley model shown in Fig. 1. The mountain profiles were calculated from the following relation for the height z as a function of the horizontal distance x , the mountain half-width a , and maximum height h . Thus,

$$z = \frac{ha^2}{(x^2 + a^2)} \quad (1)$$

Overview of the Erosion Process Observed

The sequence of events can be divided into four stages. The starting stage involves an unsteady, starting eddy, which removes

dense fluid from the downstream valley slope before traveling away with the moving fluid as shown in Fig. 2. Initially, the flow removes some of the denser fluid when the mountaintop flow has sufficient inertial force to overcome the negative buoyancy forces.

In the next stage, this initial process continues, and the height of the dense fluid eventually falls below the mountaintop, becoming partly sheltered from the shearing flow. Erosion occurs by entrainment at the top of the dense, trapped fluid. Kelvin-Helmholtz waves can occur on the leeside of the upstream mountain, but these tend to dissipate rapidly. This initial stage is shown schematically in Fig. 3.

The intermediate stage occurs next when the leeside contour of the obstacle interacts with the flow and a lee eddy forms. Figure 4 shows a schematic view of this intermediate stage. The leeside eddy continues to erode the dense valley fluid, paradoxically moving the dense fluid toward the upstream slope, where it is driven upward until it reaches the model mountaintop and is then driven downstream. During this process, an oscillation occurs in the valley fluid, either driven by the eddy, or conversely, the valley oscillation could control the eddy formation. Figure 4 shows this intermediate stage in two phases. After half a period of the valley oscillation shown in Fig. 4a, where the dense valley air has moved up the leeside slope, a vortex forms at the lee of the upstream

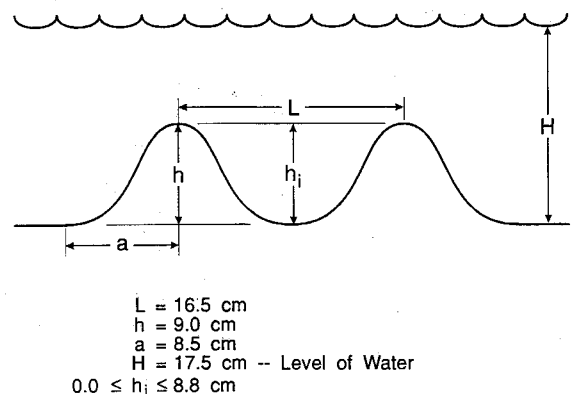


Fig. 1 Details of the Witch of Agnesi mountain profile used in scale model experiments.

Presented as Paper 92-088 at the AIAA 30th Aerospace Sciences Meeting, Reno, NV, Jan. 6-9, 1992; received July 8, 1992; revision received March 12, 1993; accepted for publication March 12, 1993. This paper is declared a work of the U.S. Government and is not subject to copyright protection in the United States.

*Graduate Student, Department of Aerospace Engineering Sciences; currently Analyst/Programmer, Hughes/STX, 4400 Forbes Blvd., Lanham, MD 20706.

†Physicist, NOAA/ERL/Wave Propagation Laboratory, 325 Broadway, Senior Member AIAA.

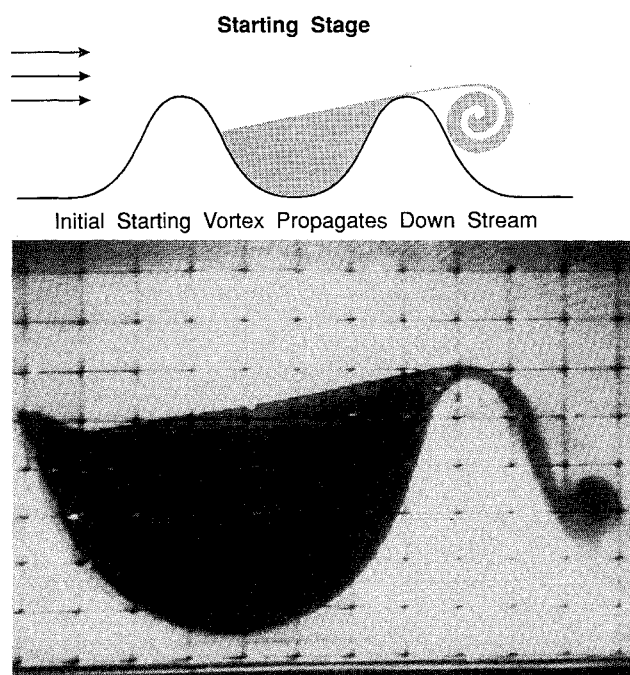


Fig. 2 Starting stage of the erosion process.

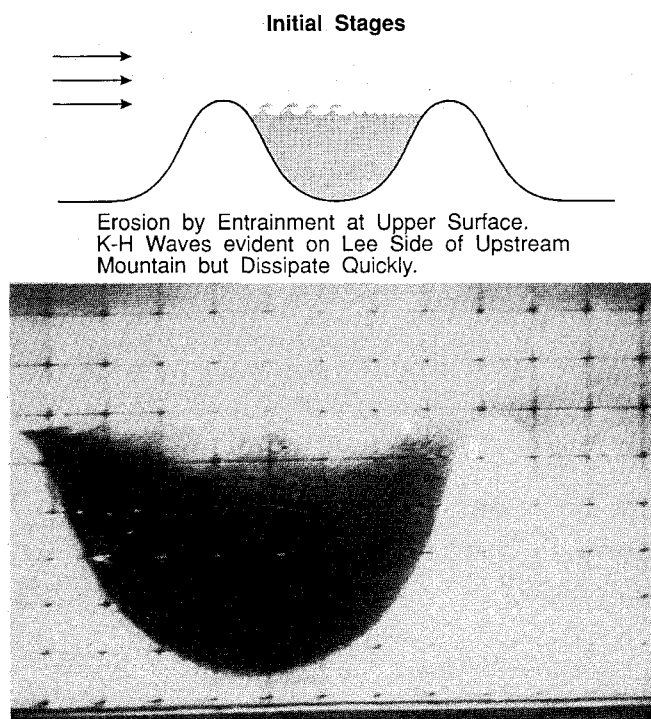


Fig. 3 Erosion by entrainment at the upper surface of the trapped fluid.

mountain. Successive vortices evacuate the inversion by forcing the dense fluid up the lee slope of the upstream mountain where it is entrained by the mountaintop shear layer and taken downstream. Some of the inversion is blown over the downstream mountaintop, but most is evacuated at the upwind side of the valley by successive vortices (Fig. 4b). Several of the figures show conceptual views of these processes and are accompanied by photographs of the laboratory experiment.

The final stage is shown schematically in Fig. 5. At this later stage, a valley oscillation or seiche is no longer apparent, and there is a drop in the rate at which the inversion is evacuated. During the final stage, the inversion is driven up the lee of the upstream mountain and no inversion fluid is pushed over the downstream mountain.

Experimental Techniques

The water in the model valley was made more dense by adding a mixture of salt, condensed milk, and food coloring. The dense fluid was syphoned into the valley, creating a stable pool of liquid clearly separated from the clear water outside. The water tunnel is a dual flow design permitting separate control of the flow in the top and bottom halves of the water tank. We slowly increased the flow speed in the top half of the tank until evacuation started. The process was monitored from the side through a grid with a video camera for after-the-fact analysis. The mountains were 12.2 cm wide and spanned the tank which was 17.5 cm high. Tests were run over a range of density increases from 2 to 10%, resulting in evacuation flow speeds ranging between 7 and 17 cm s^{-1} . The following sections summarize the results of these observations.

Experimental Results

Valley Oscillations

Haurwitz⁷ reviewed some observations of atmospheric valley oscillations and developed an analytical model for an idealized basin of cold air. In addition, many estimates of standing wave systems have been made for more complex geometries, often directed toward estimating the standing wave periods of seiche phenomena in lakes excited by earthquakes or traveling pressure disturbances. Janardhan⁸ has computed standing wave periods for a variety of geometries, and we have adapted one of these which approximates our laboratory conditions. We use a geometry of a concave, complete, parabolic basin to represent our laboratory geometry, applying a reduced gravity to account for buoyancy

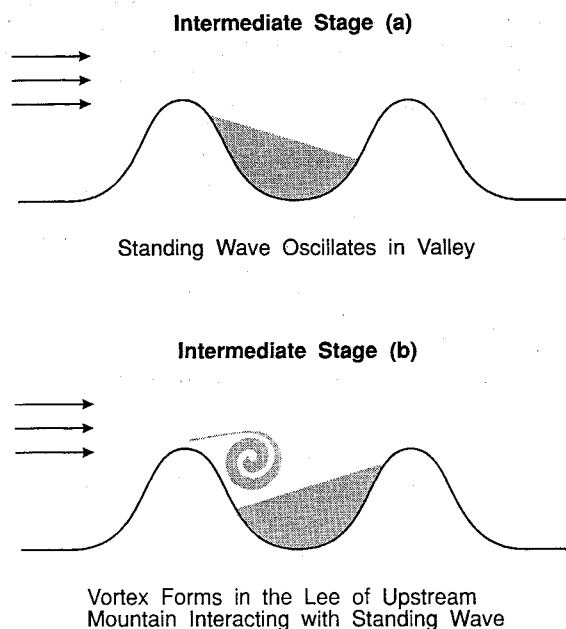


Fig. 4 Intermediate stage of erosion with standing wave present in the valley.

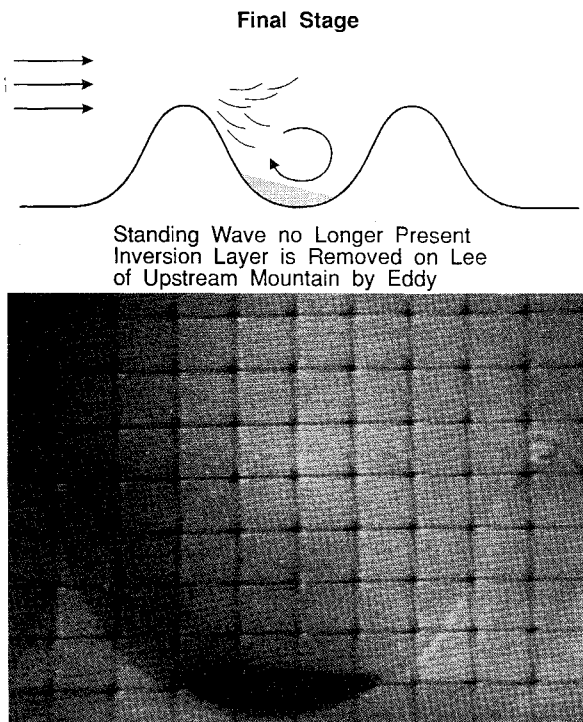


Fig. 5 Standing wave no longer present; erosion continues from leeside eddy.

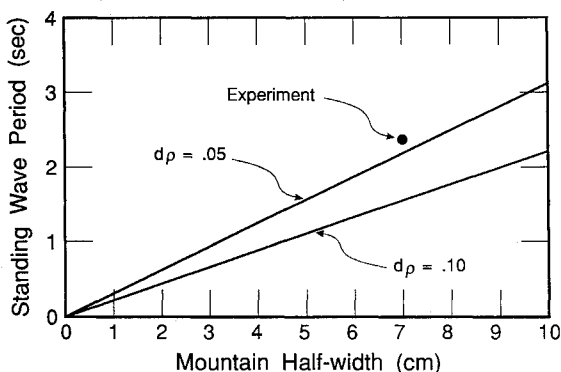


Fig. 6 Computed valley standing wave period as a function of valley half-width for two different values of density difference.

effects. The relation obtained for the period of standing wave oscillation τ is

$$\tau = \frac{2\pi a}{[N(N+1)(dp/\rho)gh_i]^{1/2}} \quad (2)$$

where a is the valley half-width, N the number of nodes, dp the density difference between the valley fluid ρ and the medium fluid, g the local gravitational acceleration, and h_i the height of the dense fluid in the valley.

The experiments were recorded with time on video tape and the images were analyzed. Figure 6 presents plots of the computed standing wave period as a function of the valley half-width for two different density differences, showing periods in the range from 1 to 3 s. The average period observed for a valley fluid height of about 7 cm and a density difference of 5% was 2.4 s and is shown on the plot. We note that for an experimental half-width of about 6 cm and an eddy circulation flow speed of about 10 cm s^{-1} , this will be about the time it takes a fluid parcel to make one complete circuit in a lee eddy. Thus, a feedback mechanism is very likely to be effective in the ventilation process.

Valley Ventilation as a Function of Time

The height of the dense fluid in the valley was measured as a function of time for different flow speeds (7, 10.5, and 13.1 cm s^{-1})

and densities (2, 5, 8, and 10%). A plot of the 2 and 5% cases as a function of time for a flow speed of 7 cm s^{-1} appears in Fig. 7. The 2% solution is eroded much faster (about 10 min) than the 5% solution (about 50 min). A region of change in slope noted on the plots occurs for both fluids. This slope change region coincided with the time at which the standing wave oscillation was no longer evident, indicating that the standing wave contributed to a more efficient erosion process. The fact that the less dense fluid was eroded more rapidly at the same flow speed is consistent with the weaker negative buoyancy forces available to provide stability. Figure 8 for density increases of 8 and 10% and a flow speed of 13.1 cm s^{-1} shows similar results. Figure 9 compares a range of density increases indicating a difficulty in obtaining repeatability for two 10% runs. This could be caused by the strong dependence of erosion rate on flow speed documented in Fig. 10, and difficulties in returning to the precise flow speed could explain the differences between the two 10% runs. In Fig. 10 for 5% solutions, there are increases in erosion times of about a factor of five as the speed was incrementally reduced from 13.1 to 7 cm s^{-1} . We interpret this (higher than anticipated) sensitivity to flow speed as caused by the presence of the lee eddy, with changes in the mean flow speed moving the recirculating parcels of fluid on or off the system resonance. A slope change was evident in all of these figures.

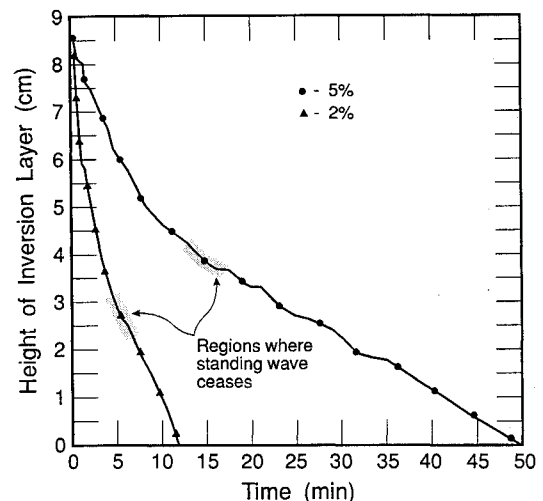


Fig. 7 Height of the dense fluid in the model valley as a function of time for a flow speed of 7 cm s^{-1} and valley fluid density increases of 2 and 5%.

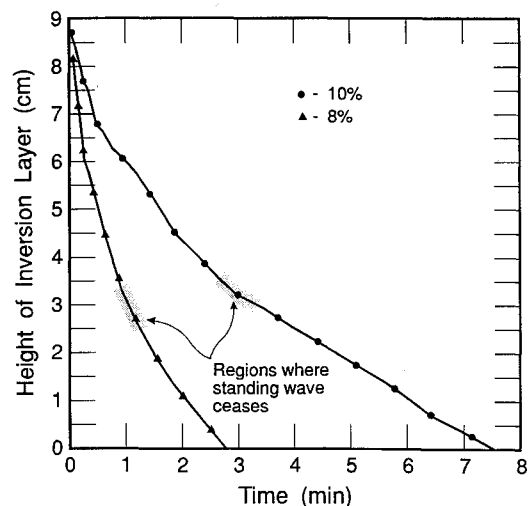


Fig. 8 Height of the dense fluid in the model valley as a function of time for a flow speed of 13.1 cm s^{-1} and valley fluid density increases of 8 and 10%.

Sensitivity to Froude Number

The Froude number is a measure of the ratio of the inertial to the gravitational forces and is defined as

$$Fr = \frac{U}{[(dp/\rho)gh_i]^{1/2}} \quad (3)$$

where U is the flow speed above the dense layer. The Froude number has been used as a criterion of the onset of erosion processes in numerical and laboratory studies,² and the value of this criterion has been verified in field measurements.^{3,4} However, these past studies did not take into account unsteady flow effects involved with complex obstacles interacting with a moving medium. In our experiments, there are several different physical processes controlling the erosion, and it may be more difficult to identify a simple criterion for onset. Specifically, the initial erosion process is dominated by horizontal shear instabilities as evidenced by the existence of Kelvin-Helmholtz waves. Following this, vortex sheets generated by flow across the upstream model mountain create circulations and excite valley oscillations, which eventually reach large amplitudes. As the dense fluid is evacuated, primarily on the leeside of the upstream mountain, the valley oscillations decrease. Finally, a large leeside eddy completes the erosion process at a slower rate, again primarily near the leeside of the peak of the upstream mountain. A value of Fr of 1.3 is suggested by the work of Bell and Thompson,² whereas Bedard³ and Bedard et al.⁴

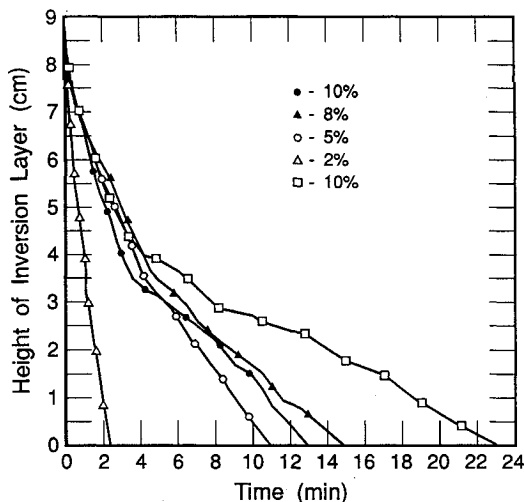


Fig. 9 Height of the dense fluid in the model valley as a function of time for a flow speed of 10.5 cm s^{-1} for a range of valley fluid density increases.

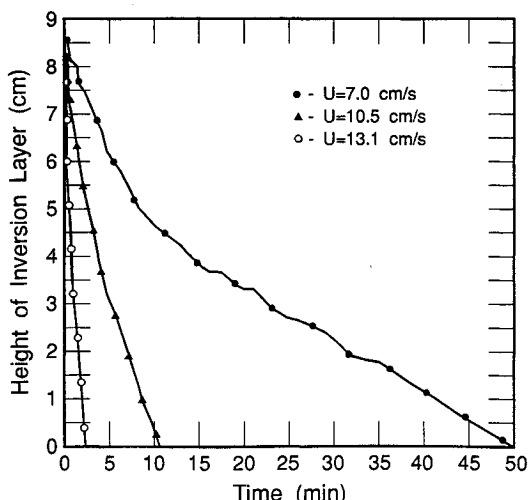


Fig. 10 Height of dense fluid in the model valley as a function of time for a valley fluid density increase of 5% and three values of flow speed, showing the strong dependence of erosion rate on flow speed.

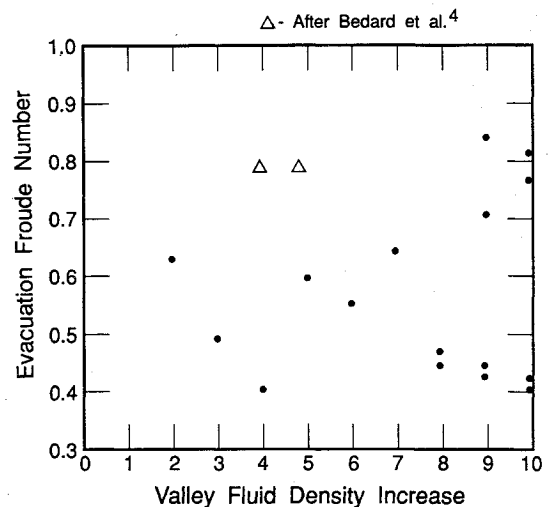


Fig. 11 Evacuation Froude number as a function of valley fluid density increase for all runs.

observed slightly smaller values (usually in the range 0.6 to 1) in the atmosphere. Bell and Thompson² indicated the existence of a rotor in their laboratory experiments under some conditions and noted the possibility for wave resonance to occur. They did not explore the implications of the existence of lee eddies.

We found that the rate of erosion was larger when the standing wave was present than after the fluid had stopped oscillating later in the process. The ratio of the two rates was typically a factor of two. We surmise that without the existence of the recirculating eddy the erosion would have ceased as the dense fluid height dropped below mountaintop height and became sheltered from the flow above.

Values of Fr were calculated for each run and appear in Fig. 11 plotted as a function of solution density difference in percent. The values of Fr at which the evacuation process started are shown in Fig. 11 plotted as a function of the fluid density difference in percent, falling in a range between 0.4 and 1.0. This is in the range of Fr observed in the atmosphere. There seems to be a trend for the experiments operated at higher densities to show more scatter. This may result from the larger inertial forces required to start the erosion process also having the potential to excite a broader range of fluid instabilities. We also note that at higher Fr more complex valley oscillations are often excited. This probably is related to more rapid flows near the mountaintop exciting higher order modes of valley oscillation.

Concluding Remarks

These model comparisons have indicated the complex series of processes involved with the evacuation of dense fluid from valleys by mountaintop flows, showing the importance of standing waves. A field experiment run by the Wave Propagation Laboratory of the National Oceanic and Atmospheric Administration⁹ provided clear evidence of the existence of such valley oscillations. Improving our ability to predict this erosion process can be important for aircraft operations, not only because of the wind shear, waves, and turbulence at the interface, but also because of the reduced visibility often accompanying a trapped pool of cold air. Also, there are often serious degradations in air quality.

We validated the use of the Froude number as a valuable index for the onset of valley evacuation. The model results obtained for valley evacuation should be valuable for numerical model experiments and provide guidance for field experiments. The Froude number also provides an index of the likelihood of a microburst penetrating an inversion layer, as shown by the scale model studies of Young et al.¹⁰ Specifically, they found that the details of microburst interaction with an inversion will depend on a Froude number defined using the height of the inversion, the density difference between the microburst and the inversion, and the speed of the microburst before impact. For $Fr < 0.6$, the microburst would

not penetrate to the surface. For Fr between about 0.6 and 1.2, the microburst would penetrate to the surface but not diverge. Above $Fr = 1.2$, significant divergence occurred.

References

- ¹Tampieri, F., and Hunt, J. C. R., "Two-Dimensional Stratified Fluid Flow Over Valleys: Linear Theory and a Laboratory Investigation," *Boundary Layer Meteorology*, Vol. 32, No. 1, 1985, pp. 257-279.
- ²Bell, R. C., and Thompson, R. O. R. Y., "Valley Ventilation by Cross Winds," *Journal of Fluid Mechanics*, Vol. 96, Pt. IV, Feb. 1980, pp. 757-767.
- ³Bedard, A. J., Jr., "Sources and Detection of Atmospheric Wind Shear," *AIAA Journal*, Vol. 20, No. 7, 1982, pp. 940-945.
- ⁴Bedard, A. J., Jr., Nagle, R., and LeFebvre, T. J., "Monostatic Acoustic Sounder Measurements During Project AEOLUS 1980: Case Studies Describing the Erosion of Surface-Based Stable Layers," *Proceedings of the International Symposium on Acoustic Remote Sensing of the Atmosphere and Oceans*, (Univ. of Calgary, Canada), Univ. of Calgary, Calgary, Alberta, Canada, 1982, pp. VI27-VI57.

⁵Neff, W. D., and Ruffieux, D., "A Model Study of Entrainment by Accelerating Ambient Winds of Nocturnal Drainage Flows and Cold Air Pools," *Proceedings of the 5th Conference Mountain Meteorology*, June 25-29, 1990 (Boulder, CO), American Meteorological Society, Boston, MA, 1990, pp. 289-295.

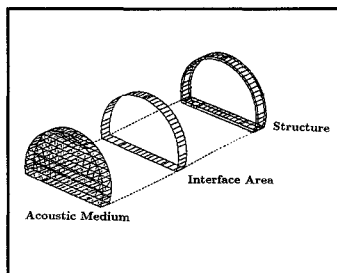
⁶Durran, D., "Another Look at Downslope Windstorms. Part 1: The Development of Analogs to Supercritical Flow in an Infinitely Deep, Continuously Stratified Fluid," *Journal of Atmospheric Sciences*, Vol. 43, No. 21, 1986, pp. 2527-2543.

⁷Haurwitz, B., "Oscillations in a Basin of Cold Air," *Atmosphere*, Vol. 11, No. 4, 1973, pp. 141-144.

⁸Janardhan, S., "Some Computations on Seiches in Lake Fife at Khadakvasla, Poona," *Indian Journal of Meteorology and Geophysics*, Vol. 10, No. 1, 1959, pp. 265-274.

⁹Bedard, A. J., Jr., "Infrasound Originating Near Mountainous Regions in Colorado," *Journal of Applied Meteorology*, Vol. 16, No. 7, 1978, pp. 1049-1055.

¹⁰Young, J. W., III, Lane, F. D., and Bedard, A. J., Jr., "The Effect of a Ground-Based Inversion Layer on an Impacting Microburst," *AIAA Aerospace Sciences Meeting*, AIAA Paper 89-0810, Reno, NV, Jan. 1989.



Theoretical and Computational Methods in Structural Acoustics

October 28-29, 1993
Long Beach, California

This Continuing Education Short Course is being offered in conjunction with the 15th AIAA Aeroacoustics Conference in Long Beach, California

THIS course provides a comprehensive introduction to the concepts, principles, and application of theoretical and computational methods in structural acoustics dealing with the problem of interaction of structures with sound and other dynamic disturbances. The focus will be on basic principles as well as some of the advances in the field of structural acoustics and how they relate to practical problems. Find out how to conduct a more cost-effective structural acoustic analysis of periodic systems by combining the finite element method with the periodic structure theory.



American Institute of
Aeronautics and Astronautics

FAX or call David Owens, Phone 202/646-7447, FAX 202/646-7508 for more information.